atmosphere

MDPI

Article

Tri-Base Synergy in Sulfuric Acid-Base Clusters

Hong-Bin Xie [1] **and Jonas Elm** [2,*]

[1] Key Laboratory of Industrial Ecology and Environmental Engineering (Ministry of Education), School of Environmental Science and Technology, Dalian University of Technology, Dalian 116024, China; hbxie@dlut.edu.cn

[2] Department of Chemistry and iClimate, Aarhus University, 8000 Aarhus, Denmark

* Correspondence: jelm@chem.au.dk

Abstract: Synergistic effects between different bases can greatly enhance atmospheric sulfuric acid (SA)-base cluster formation. However, only the synergy between two base components has previously been investigated. Here, we extend this concept to three bases by studying large atmospherically relevant $(SA)_3(base)_3$ clusters, with the bases ammonia (A), methylamine (MA), dimethylamine (DMA), trimethylamine (TMA) and ethylenediamine (EDA). Using density functional theory—ωB97X-D/6-31++G(d,p)—we calculate the cluster structures and vibrational frequencies. The thermochemical parameters are calculated at 29,815 K and 1 atm, using the quasi-harmonic approximation. The binding energies of the clusters are calculated using high level DLPNO-CCSD(T_0)/aug-cc-pVTZ. We find that the cluster stability in general depends on the basicity of the constituent bases, with some noteworthy additional guidelines: DMA enhances the cluster stability, TMA decreases the cluster stability and there is high synergy between DMA and EDA. Based on our calculations, we find it highly likely that three, or potentially more, different bases, are involved in the growth pathways of sulfuric acid-base clusters.

Keywords: atmospheric molecular clusters; new particle formation; aerosols; quantum chemistry

Citation: Xie, H.-B.; Elm, J. Tri-Base Synergy in Sulfuric Acid-Base Clusters. *Atmosphere* **2021**, *12*, 1260. https://doi.org/10.3390/atmos12101260

Academic Editor: Luís Pedro Viegas

Received: 26 August 2021
Accepted: 23 September 2021
Published: 27 September 2021

1. Introduction

Atmospheric aerosol particles have ubiquitous effects on our global climate, by scattering sunlight away from the surface of the Earth [1] and acting as seeds for cloud formation [2]. Based on modelling studies, up to half the number of formed cloud condensation nuclei (CCN) are believed to be formed from atmospheric new particle formation (NPF) [3]. Vapour molecules with strong intermolecular interactions can form molecular clusters in the atmosphere via hydrogen bond formation or ionic interactions. Small clusters can continuously form and break-up, and their survival to larger sizes depends on the attachment of additional molecules [4]. When reaching a certain size, the cluster contains enough intermolecular interactions to suppress the evaporation of its components, leading to NPF.

Sulfuric acid (SA) is known to be an essential component in NPF in many regions [5], but, additional stabilizing compounds are required to facilitate the cluster formation process. Abundant atmospheric bases such as ammonia (A) are considered a principal stabilizer of sulfuric acid clusters [6–9], but sulfuric acid–ammonia cluster formation cannot by itself explain observed NPF events [10]. Stronger, less abundant bases such as amines have been shown to efficiently stabilize sulfuric acid clusters [11]. Currently, more than 150 amines have been detected in the ambient atmosphere [12,13]. The simple alkylamines such as methylamine (MA), dimethylamine (DMA) and trimethylamine (TMA) [13–19] and diamines, such as ethylenediamine (EDA), putrescine and cadaverine, have been shown to significantly enhance SA-base NPF compared to ammonia [20–23].

Electrically neutral SA-base clusters have been shown to be most stable when consisting of an equal amount of acids and base molecules–$(SA)_n(base)_n$ [24,25]. Clusters with one more acid than base molecule—$(SA)_{n+1}(base)_n$—are generally more stable than the corresponding

clusters with one more base than acid molecule—$(SA)_n(base)_{n+1}$. In most cases, the cluster formation pathways follow a mechanism that alternately adds an SA and a base molecule. For systems that are strongly bound, collisions between clusters and the $(SA)_1(base)_1$ dimer are also involved in the growth. This implies that the $(SA)_n(base)_n$ clusters are usually involved in the cluster formation pathway leading to NPF. Furthermore, it has previously been demonstrated that the $(SA)_3(base)_3$ clusters have low evaporation rates, even when consisting of weaker bases such as A or MA [25]. Hence, the $(SA)_3(base)_3$ clusters or larger, can generally be considered stable under tropospheric conditions (218.15–298.15 K).

The potency of SA-base cluster formation has, in many cases, been correlated with the basicity of the clustering base [25,26]. However, recent evidence suggests that there is a synergistic effect between different bases compounds, such as the SA-A-DMA system, leading to enhanced NPF rates compared to the isolated SA-A and SA-DMA systems [27–29]. However, at the moment, the concept of base synergy in SA-driven cluster formation has only been elucidated using two bases compounds. Here, we extend this concept to three bases to explore the potential tri-base synergy in SA-base clusters. To represent clusters that are relevant for the formation pathways leading to NPF in SA-base clustering we herein study the $(SA)_3(base)_3$ cluster systems. We study all combinations of tri-base clusters with the bases ammonia (A), methylamine (MA), dimethylamine (DMA), trimethylamine (TMA) and ethylenediamine (EDA).

2. Methods

2.1. Computational Details

The Gaussian 16 program [30] suite was employed for all semi-empirical and density functional theory calculations, applying the Gaussian 09 default convergence criteria to allow comparison with the existing data in the Atmospheric Cluster DataBase (ACDB) [31]. Domain based local pair natural orbital DLPNO-CCSD(T_0) [32,33] single point energy calculations were calculated using the ORCA 4.2.1 program [34,35], with a TightSCF convergence. Vibrational frequencies with low wavenumbers can be a significant source of errors when calculating the vibrational entropy using the harmonic oscillator approximation. Using the Goodvibes [36] program, we applied the quasi-harmonic approximation [37], where the entropy contribution for vibrations below 100 cm^{-1} cutoff are calculated with the formula for the rotational entropy instead. The final binding free energies are calculated at the DLPNO-CCSD(T_0)/aug-cc-pVTZ//ωB97X-D/6-31++G(d,p)level of theory. This level of theory has previously been recommended for studying atmosphere molecular clusters [38,39], based on extensive benchmarks on atmospheric relevant cluster systems [40–42].

The configurational sampling of the cluster structures is performed based on well-established protocols [27,43,44] and is similar to our recently applied workflow [45,46]:

$$\text{ABCluster} \rightarrow \text{PM7} \rightarrow \text{sort} \rightarrow \text{DFT} \rightarrow \text{restart} \rightarrow \text{sort} \rightarrow \text{DLPNO}$$

In the ABCluster calculations, we sampled the clusters using both neutral as well as anionic and cationic monomers, to simulate bond breaking in the clusters. We only allowed a single proton transfer from sulfuric acid to the bases, leading to four different protonation states by either having neutral monomers or 1–3 proton transfers. Including different monomer protonation states in the sampling leads to a much more elaborate exploration of the potential energy surface of the clusters. When different bases could act as proton acceptors, the base with the highest basicity was protonated. For each protonation state of the clusters we saved 1000 local minima, leading to 4000 PM7 calculations for each cluster system. After the PM7 optimization we pair-wise sort the cluster configurations and remove duplicates based the on root mean square deviations (RMSD) between atomic positions. We applied the ArbAlign [47] program to align the cluster configurations and configurations are treated as unique if the structures have a RMSD above 0.38 Å. This value is based on previous experience with sulfuric acid-water clusters [48] and might be a bit strict for the much more strongly bound SA-base clusters studied here. Unique conformations were subsequently optimized, and vibrational frequencies were calculated at the ωB97X-D/6-31++G(d,p) level

of theory. It was confirmed that there were no imaginary frequencies after the ωB97X-D/6-31++G(d,p) calculation. The DFT calculations were restarted up to three times, due to a to poor initial starting geometry from the PM7 calculations, to lead to full convergence of the majority of the configurations. After the DFT calculations the clusters are again sorted based on RMSD. In case of the $(SA)_3(EDA)_3$ system, we obtained too many different configurations (1125) to sort all the structures directly, as very few duplicates existed. Based on the free energy ordered configurations, we divided the set of clusters into three different subsets. Each subset was then individually sorted and combined afterwards. While unlikely, this implies that we might have a few cluster configurations between the different subsets that are identical. Finally, DLPNO-CCSD(T_0)/aug-cc-pVTZ single point energies are calculated on top of the DFT geometries for the five lowest free energy cluster configurations.

2.2. Tri-Base Synergistic Effects

We previously described a synergistic effect between two cluster components as thermochemistry that lead to a highly non-additive behaviour with synergy factor $\Gamma_{j,k}$ between component j and k defined as [45,46]:

$$\Gamma_{j,k} = \Delta G_{\text{bind},i\ldots j,k,\ldots,n} - \left(\frac{\Delta G_{\text{bind},i\ldots j,j,\ldots,n} + \Delta G_{\text{bind},i\ldots k,k,\ldots,n}}{2} \right). \quad (1)$$

In this formulation, the synergy factor corresponds to the difference in free energy (in kcal mol^{-1}) between a cluster that consists of components j,k compared to the average of the corresponding clusters that consist of j,j and k,k. A negative synergy factor indicates a synergistic effect (a decrease in the binding free energy), while a positive synergy factor indicates a dyssynergistic effect (an increase in the binding free energy). Here, we extend this concept to three components j,k,l and calculate the tri-base synergy factor $\Gamma_{j,k,l}$ as follows.

$$\Gamma_{j,k,l} = \Delta G_{\text{bind},i\ldots j,k,l,\ldots,n} - \left(\frac{\Delta G_{\text{bind},i\ldots j,j,j,\ldots,n} + \Delta G_{\text{bind},i\ldots k,k,k,\ldots,n} + \Delta G_{\text{bind},i\ldots l,l,l,\ldots,n}}{3} \right). \quad (2)$$

Similarly to the two component cases, the $\Gamma_{j,k,l}$ synergy factor corresponds to the difference in free energy (in kcal mol^{-1}) between a cluster that consists of components j,k,l compared to the average of the corresponding clusters that consist of j,j,j and k,k,k and l,l,l.

3. Results and Discussion

3.1. Cluster Structures

We studied $(SA)_3(base)_3$ clusters, with five different bases (ammonia (A), methylamine (MA), dimethylamine (DMA), trimethylamine (TMA) and ethylenediamine (EDA)). Applying the sampling methodology outlined above we identified a total of 5140 unique cluster structures. Figure 1 presents the identified lowest free energy (298.15 K and 1 atm) cluster structures at the ωB97X-D/6-31++G(d,p) level of theory.

The $(SA)_3(A)_3$, $(SA)_3(MA)_3$ and $(SA)_3(DMA)_3$ clusters have previously been studied in the literature, while $(SA)_3(TMA)_3$ and $(SA)_3(EDA)_3$ clusters are new. Compared to the clusters available from the Atmospheric Cluster Database (ACDB) [31], we here identify an $(SA)_3(A)_3$ cluster and an $(SA)_3(MA)_3$ cluster which are 1.25 and 1.10 kcal mol^{-1} lower in free energy, respectively. We identified the same lowest free energy $(SA)_3(DMA)_3$ cluster as the one in the ACDB. The fact that we identify the same or lower free energy cluster structures compared to previous studies further validates the configurational sampling approach applied in this work.

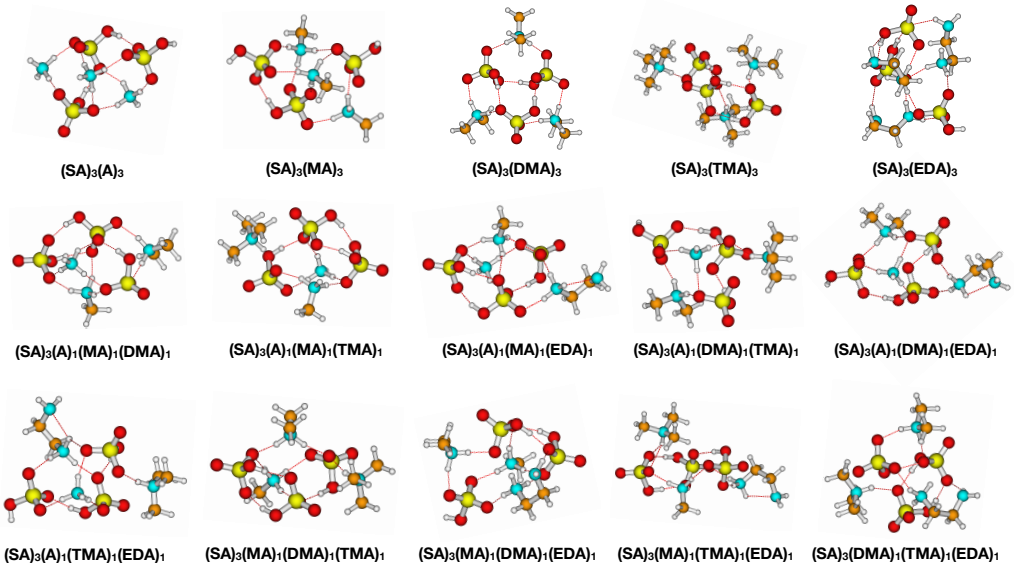

Figure 1. The identified lowest free energy cluster structures (at 298.15 K and 1 atm) at the ωB97X-D/6-31++G(d,p) level of theory.

In all clusters, we observe a proton transfer from sulfuric acid to each base, effectively yielding bisulfate-ammonium/amminium cluster structures. For the weaker bases (A, MA) and EDA, we observe 1–2 vacant S–OH hydrogen bond donor groups at the exterior of the clusters. Despite having two available proton acceptor groups, we do not observe sulfate ion formation in the $(SA)_3(EDA)_3$ clusters. This is in contrast to previous studies of diamines with a longer carbon atom linker between the amino groups, such as putrescine [22]. For the very strong bases (DMA and TMA) the most favourable cluster structure has a bisulfate core, where all S-OH hydrogen bond donors are involved in bisulfate-bisulfate interactions. In the $(SA)_3(DMA)_3$ cluster the base molecules link the bisulfate units via the S=O acceptor groups. This linkage is not possible in the $(SA)_3(TMA)_3$ cluster, as there is only a single hydrogen bond donor available in TMA. In the $(SA)_3(TMA)_3$ cluster we also observe S=O $\cdots$ H–C weak interactions with the hydrogen atoms from the methyl groups in the TMA molecules.

For the mixed base clusters, we only identify vacant S-OH groups in clusters that either have A or MA present. For most clusters containing EDA, the additional amine group preferentially forms an intramolecular interaction instead of further interacting with the bisulfate ions. Such secondary intramolecular interactions have previously been identified in sulfuric acid–diamine clusters [21]. For all the mixed base clusters containing TMA, the TMA molecule resides at the periphery of the cluster, only interacting via one strong N-H donor and 1–2 weak S=O $\cdots$ H-C interactions.

3.2. Thermochemistry

The thermochemistry of the $(SA)_3(base)_3$ clusters was calculated at the DLPNO-CCSD(T_0)/aug-cc-pVTZ//ωB97X-D/6-31++G(d,p) level of theory. We applied the quasi-harmonic approximation where vibrational frequencies below 100 cm^{-1} were calculated using the rotational partition function instead of the vibrational partition function. Table 1 presents the calculated binding free energies (ΔG), binding enthalpies (ΔH) and binding entropies (ΔS). The free energies were calculated at 298.15 K and 1 atm, corresponding to tropospheric conditions at the surface. The free energy can easily be re-calculated at any atmospheric temperature under the assumption that ΔH and ΔS do not change considerably with temperature. Table 1 also tabulates the calculated free energy at the tropopause corresponding to roughly 10 km and a temperature of 218.15 K. The classifications, weak (w), medium (m) and strong (s), refer to the gas-phase basicity of the bases in the clusters, based on the work by Hunter et al. [49].

Table 1. Calculated binding free energies (at 298.15/218.15 K, 1 atm) of the $(SA_3)(base)_3$ clusters at the DLPNO-CCSD(T_0)/aug-cc-pVTZ//ωB97X-D/6-31++G(d,p) level of theory using the quasi-harmonic approximation. $\Delta G_{298.15K}$, $\Delta G_{218.15K}$ and ΔH are in kcal mol^{-1}. ΔS are in cal mol^{-1} K^{-1}. The classifications refer to the base strength, with w = weak, m = medium and s = strong.

	Classification	$\Delta G_{298.15K}$	$\Delta G_{218.15K}$	ΔH	ΔS
$(A)_3$	w,w,w	−51.5	−66.6	−107.9	−189.2
$(MA)_3$	m,m,m	−66.0	−82.0	−125.5	−199.7
$(DMA)_3$	s,s,s	−75.5	−92.2	−137.9	−209.2
$(EDA)_3$	s,s,s	−74.4	−92.1	−140.4	−221.5
$(TMA)_3$	s,s,s	−64.8	−82.0	−128.7	−214.2
$(A)_1(MA)_1(DMA)_1$	w,m,s	−65.2	−81.0	−124.2	−198.0
$(A)_1(MA)_1(EDA)_1$	w,m,s	−64.2	−80.7	−125.6	−205.8
$(A)_1(MA)_1(TMA)_1$	w,m,s	−62.3	−78.2	−121.4	−198.4
$(A)_1(DMA)_1(EDA)_1$	w,s,s	−68.4	−84.9	−130.0	−206.8
$(A)_1(DMA)_1(TMA)_1$	w,s,s	−65.6	−82.0	−126.5	−204.3
$(A)_1(TMA)_1(EDA)_1$	w,s,s	−63.2	−79.7	−124.6	−205.8
$(MA)_1(DMA)_1(TMA)_1$	m,s,s	−70.7	−87.6	−133.7	−211.4
$(MA)_1(DMA)_1(EDA)_1$	m,s,s	−73.3	−90.1	−135.9	−209.9
$(MA)_1(TMA)_1(EDA)_1$	m,s,s	−71.0	−88.0	−134.2	−211.9
$(DMA)_1(TMA)_1(EDA)_1$	s,s,s	−72.2	−89.4	−136.1	−214.3

As cluster formation is accompanied by a decrease in both ΔH and ΔS, the free energies will be lower at lower temperatures, leading to more stable clusters. This is consistent with the binding free energies reported in Table 1. The following discussion will be based on the free energies calculated at 298.15 K and unless otherwise specified. For the $(SA)_3(base)_3$ clusters, with a single type of base, the thermochemistry to some extent follow the gas-phase basicity of the bases, except for the $(SA)_3(TMA)_3$ cluster. We observe the following ranking of the cluster binding free energies (in kcal mol^{-1}): $(A)_3$ (−51.5) < $(TMA)_3$ (−64.8) < $(MA)_3$ (−66.0) < $(EDA)_3$ (−74.4) < $(DMA)_3$ (−75.5). It was recently shown for the $(SA)_1(base)_1$ dimer clusters that $(SA)_1(TMA)_1$ ($\Delta G = -12.6$ kcal mol^{-1}) was slightly more stable than $(SA)_1(DMA)_1$ ($\Delta G = -11.5$ kcal mol^{-1}) [45]. However, for the $(SA)_2(base)_2$ clusters the stability switches such that the $(SA)_2(DMA)_2$ cluster ($\Delta G = -44.0$ kcal mol^{-1}) is more stable than the corresponding $(SA)_2(TMA)_2$ cluster ($\Delta G = -41.5$ kcal mol^{-1}) [45]. This trend is further illustrated herein by the calculated low stability of the $(SA)_3(TMA)_3$ cluster ($\Delta G = -64.8$ kcal mol^{-1}) compared to the $(SA)_3(DMA)_3$ cluster ($\Delta G = -75.5$ kcal mol^{-1}). The low stability of the $(SA)_3(TMA)_3$ cluster can be understood from the lack of available hydrogen bond donors in TMA, as seen from the emerging weak S=O $\cdots$ H-C interactions. The $(SA)_3(EDA)_3$ cluster ($\Delta G = -74.4$ kcal mol^{-1}) is found to be close in stability to the $(SA)_3(DMA)_3$ cluster, with a difference of only 1.1 kcal mol^{-1}. This is in contrast to the recent finding for the smaller $(SA)_2(base)_2$ clusters, where the $(SA)_2(EDA)_2$ cluster was found to be 2.2 kcal mol^{-1} higher in free energy compared to the $(SA)_2(DMA)_2$ cluster [45]. This could indicate that as the clusters become larger, diamines might further improve the stability of the cluster. This makes sense from a structural perspective, as attachment to a larger cluster will lead to less strain in the carbon backbone of the diamines.

The mixed clusters containing ammonia are seen to have the following ranking in binding free energy (in kcal mol^{-1}): $(A)_1(MA)_1(TMA)_1$ (−62.3) < $(A)_1(TMA)_1(EDA)_1$ (−63.2) < $(A)_1(MA)_1(EDA)_1$ (−64.2) < $(A)_1(MA)_1(DMA)_1$ (–65.2) < $(A)_1(DMA)_1(TMA)_1$ (−65.6) < $(A)_1(DMA)_1(EDA)_1$ (−68.4). Again we see the general trend of clusters containing TMA being less stable, except when a DMA molecule is also present. The $(SA)_3(A)_1(DMA)_1(EDA)_1$ cluster is significantly (∼3 kcal mol^{-1}) more stable then the remaining clusters containing ammonia.

The stability of the remaining mixed clusters have the following ranking in the binding free energies (in kcal mol^{-1}): $(MA)_1(DMA)_1(TMA)_1$ (−70.7) < $(MA)_1(TMA)_1(EDA)_1$ (−71.0) < $(DMA)_1(TMA)_1(EDA)_1$ (−72.2) < $(MA)_1(DMA)_1(EDA)_1$ (−73.3). All four clus-

ters are relatively close in stability, but some trends are possible to deduce. Again, having both DMA and EDA in the cluster leads to the highest stability. Similarly, having TMA present generally leads to a slight decrease in the stability. The high stability when having both DMA and EDA present in sulfuric acid clusters was also observed previously for the smaller $(SA)_2(DMA)_1(EDA)_1$ clusters [45]. This is consistent with the calculated free energies in Table 1. For instance, it is seen that the clusters that consist of both DMA and EDA are in all cases some of the most stable ones. Overall, it is still found that DMA leads to the most stable clusters. While the calculated free energies are lower at lower temperatures, the above stability rankings were generally found to be independent of whether the free energy was calculated at 298.15 K or 218.15 K.

To look further into the thermochemistry of the mixed base clusters, we can calculate the tri-base synergy factors using Equation (2). Table 2 presents the calculated synergy factors at the DLPNO-CCSD(T_0)/aug-cc-pVTZ//ωB97X-D/6-31++G(d,p) level of theory using the quasi-harmonic approximation, at 298.15 K and 218.15 K at a reference pressure of 1 atm.

Table 2. Calculated tri-base synergy factors (at 298.15/218.15 K, 1 atm) of the mixed $(SA)_3(base)_3$ clusters at the DLPNO-CCSD(T_0)/aug-cc-pVTZ//ωB97X-D/6-31++G(d,p) level of theory using the quasi-harmonic approximation. Data are presented in in kcal mol^{-1}.

	298.15 K	**218.15 K**
$\Gamma_{A,MA,DMA}$	−0.8	−0.7
$\Gamma_{A,MA,EDA}$	−0.3	−0.5
$\Gamma_{A,MA,TMA}$	−1.5	−1.3
$\Gamma_{A,DMA,EDA}$	−1.2	−1.3
$\Gamma_{A,DMA,TMA}$	−1.7	−1.7
$\Gamma_{A,TMA,EDA}$	0.3	0.5
$\Gamma_{MA,DMA,TMA}$	−1.9	−2.2
$\Gamma_{MA,DMA,EDA}$	−1.3	−1.3
$\Gamma_{MA,TMA,EDA}$	−2.6	−2.6
$\Gamma_{DMA,TMA,EDA}$	−0.7	−0.6

We see very little difference in whether the synergy factors were calculated at 298.15 K or 218.15 K. Hence, in the following we will only discuss the 298.15 K results. In all cases, we see a synergetic effect between the base components, except for the $(SA)_3(A)_1(TMA)_1(EDA)_1$ cluster. The synergy factors range from −2.6 to 0.3 kcal mol^{-1}. The lowering of the free energy of the clusters compared to the average of the isolated systems, indicates that it is likely that some of the clusters will exist with multiple bases present. The synergy factor also gives insight into how favourable it is to exchange base types. For instance, due to the very low stability of the $(SA)_3(TMA)_3$ clusters, the clusters containing TMA have favourable synergy factors. Hence, the synergy factors indicate that sulfuric acid-base clusters could likely contain a mix of different bases.

As also illustrated by the discussion above, the thermochemistry does to some extent (except for TMA) follow the classifications, that is, the basicity of clustering bases. For instance, clusters which consist of one weak, one medium and one strong base (the w,m,s classification) exhibit thermochemistry with similar values, from −62.3 to −65.2 kcal mol^{-1}. Exchanging the medium (MA) base with a strong base (DMA,TMA,EDA) from w,m,s to w,s,s increases the stability slightly, with binding free energies in the range from −63.2 to −68.4 kcal mol^{-1}. Exchanging the weak base for a medium base from w,s,s to m,s,s is seen to further increase the stability of the clusters with binding free energies in the range from −70.7 to −73.3 kcal mol^{-1}. Hence, in general the cluster stabilities follow the classifications, but we can set up a few fundamental additional guidelines for the thermochemistry of the $(SA)_3(base)_3$ clusters:

- Clusters containing DMA have the highest stability;
- Having TMA present generally leads to a slight decrease in the cluster stability;

- There is high synergy between DMA and EDA.

The potential to form strongly bound sulfuric acid-base clusters can be attributed to three different contributions: (1) the basicity of the base [14]; (2) the hydrogen bond capacity of the base [50] (i.e., how many N-H donors); and (3) sterical hindrance [27]. This is in excellent agreement with the outlined guidelines. DMA has a perfect balance between all these components, while TMA suffers due to a low hydrogen bond capacity. The diamine EDA shows high synergy due to an increased hydrogen bond capacity due to its two amino groups. In general, steric hindrance in sulfuric acid clusters can be expected to be small, but might have an influence if, for instance, some of the sulfuric acid molecules were exchanged with methanesulfonic acid (MSA) [51]. These guidelines for the thermochemistry can be visualized by plotting the calculated free energies of the clusters (at 298.15 K, 1 atm) as a function of the sum of gas-phase basicities of the constituent bases (see Figure 2).

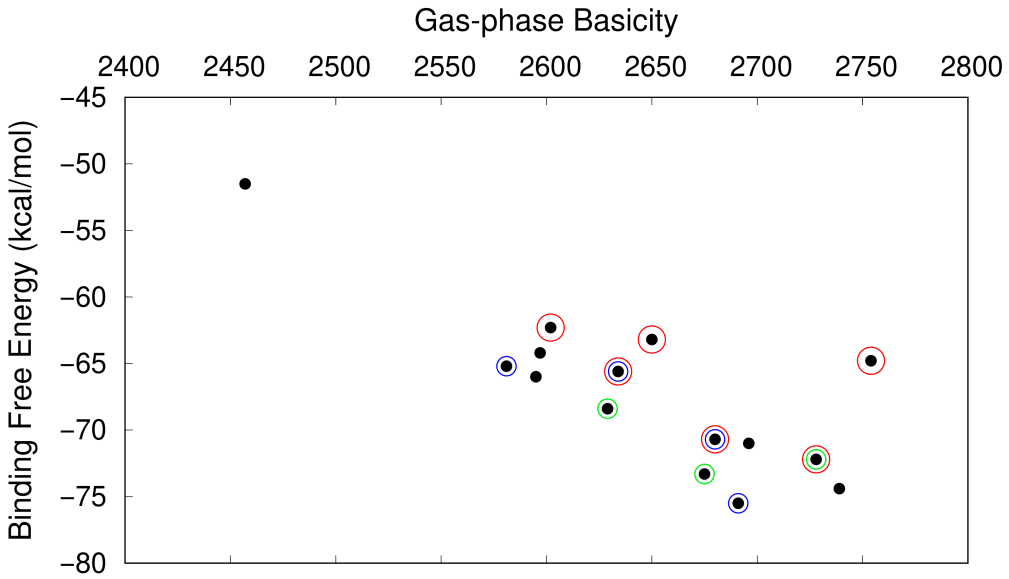

Figure 2. Correlation between the basicity of the clusters and the calculated binding free energies (at 298.15 K, 1 atm). The red circle indicates that TMA is present, the green circle includes DMA and includes both DMA and EDA.

The fact that the thermochemistry to some degree follows the classification of the clusters allows us, as a rough approximation, to use the thermochemistry presented in Table 1 for unknown $(SA)_3(base)_3$ cluster systems, while also keeping the above guidelines in mind. A similar conclusion was previously found for the smaller $(SA)_{1–2}(base)_{1–2}$ cluster systems [45], but for the smaller clusters thereno significant synergy between the clustering bases was observed.

4. Concentrations

While the thermochemistry provides some information about the cluster compositions, we also have to take the concentration of the clustering species onto account. The equilibrium concentration of a $(SA)_3(base)_3$ cluster is given by:

$$[(SA)_3(base)_3] = [base(1)][base(2)][base(3)][SA]^3 \exp\left(-\frac{\Delta G}{RT}\right). \quad (3)$$

Here, ΔG is the binding free energy of the $(SA)_3(base)_3$ cluster, R is the gas constant and T is the temperature. Here we will use the weakest bound $(SA)_3(A)_3$ cluster system as a reference. That is, we will see how much the mixed base clusters enhance the cluster

equilibrium concentration compared to the corresponding ammonia clusters. Dividing by the concentration of $(SA)_3(A)_3$ clusters, we obtain:

$$\frac{[(SA)_3(base)_3]}{[(SA)_3(A)_3]} = \frac{[base(1)][base(2)][base(3)]}{[A]^3} \exp\left(-\frac{\Delta\Delta G}{RT}\right), \quad (4)$$

where $\Delta\Delta G$ is the free energy difference between a given $(SA)_3(base)_3$ cluster and the $(SA)_3(A)_3$ cluster. We will use the following representative mixing ratios for the concentrations of the different species: A (10 ppb), MA (100 ppt), DMA (10 ppt), TMA (10 ppt) and EDA (10 ppt). These values correspond to the high limit applied in our recent work [45,46]. As the sulfuric acid ammonia system has been shown to be very dependent on ions, the $(SA)_3(A)_3$ concentration can be expected to be significantly underestimated from our calculations compared to the experimental results. Experimentally, it has been determined that SA-DMA is three orders of magnitude more efficient in forming new particles compared to SA-A. Hence, we rescaled the results such that this ratio between the concentration of SA-A and SA-DMA clusters is correct. Table 3 presents the scaled relative cluster equilibrium concentrations compared to the $(SA)_3(A)_3$ cluster.

Table 3. Calculated scaled relative cluster equilibrium concentration compared to the $(SA)_3(A)_3$ cluster.

	Relative Concentration
$(MA)_3$	1.1×10^{-1}
$(DMA)_3$	1.0×10^{3}
$(EDA)_3$	1.5×10^{2}
$(TMA)_3$	1.5×10^{-5}
$(A)_1(MA)_1(DMA)_1$	2.6×10^{-1}
$(A)_1(MA)_1(EDA)_1$	5.3×10^{-2}
$(A)_1(MA)_1(TMA)_1$	2.0×10^{-3}
$(A)_1(DMA)_1(EDA)_1$	5.8
$(A)_1(DMA)_1(TMA)_1$	5.7×10^{-2}
$(A)_1(TMA)_1(EDA)_1$	1.0×10^{-3}
$(MA)_1(DMA)_1(TMA)_1$	2.8
$(MA)_1(DMA)_1(EDA)_1$	2.4×10^{2}
$(MA)_1(TMA)_1(EDA)_1$	5.1
$(DMA)_1(TMA)_1(EDA)_1$	4.0

As cluster growth pathways of sulfuric acid-base systems usually involve the clusters with a 1:1 ratio of acids to bases, it can be assumed that the $(SA)_3(base)_3$ clusters are most likely involved in the formation of new particles. As the SA-DMA system is known to form stable clusters at the kinetic limit [52], we can use the relative concentration of $(SA)_3(DMA)_3$ as an indicator for systems that might be involved in NPF. We see that all the studied systems are below the relative concentration of the $(SA)_3(DMA)_3$ cluster. However, the $(SA)_3(MA)_1(DMA)_1(EDA)_1$ and the $(SA)_3(EDA)_3$ cluster systems are within a factor ~10 of the $(SA)_3(DMA)_3$ cluster system. While this is inferred evidence, it could indicate that these cluster systems will have a non-negligible contribution to the cluster formation pathways under ambient atmospheric conditions and thereby might contribute to NPF. Similarly, we see that the $(SA)_3(A)_1(DMA)_1(EDA)_1$, $(SA)_3(MA)_1(DMA)_1(TMA)_1$, $(SA)_3(MA)_1(TMA)_1(EDA)_1$ and $(SA)_3(DMA)_1(TMA)_1(EDA)_1$ cluster systems are within a factor ~100 of the $(SA)_3(DMA)_3$ system. Hence, these systems might also make a minor contribution to the formation pathways of the sulfuric acid-base clusters.

Interestingly, we see that the concentration of the $(SA)_3(TMA)_3$ clusters is more or less equal to the $(SA)_3(A)_3$ cluster system. As SA and A alone cannot explain the observed new particle formation rates, it is very likely that TMA clusters by themselves do not contribute significantly to NPF. However, TMA might still contribute to the overall cluster formation

pathways as the very initial $(SA)_1(TMA)_1$ cluster is very stable [45] and TMA is included in some of the mixed base clusters. Based on these findings, it is highly likely that numerous different bases are involved in NPF in the ambient atmosphere.

5. Conclusions

We have investigated $(SA)_3(base)_3$ cluster formation, with the bases ammonia (A), methylamine (MA), dimethylamine (DMA), trimethylamine (TMA) and ethylenediamine (EDA), with a focus on identifying potential synergistic effects between the bases. We identify that the cluster stability primarily depends on the basicity of the constituent bases with the following trends: DMA enhances the cluster stability, TMA decreases the cluster stability and there is high synergy between DMA and EDA. Hence, it might be worth further investigating the competing effects of DMA and TMA in larger mixed SA-DMA-TMA clusters. Furthermore, larger cluster SA-DMA-EDA cluster systems should also be investigated.

Based on both the calculated thermochemistry and relative cluster equilibrium concentration estimates, it is clear that there is a synergistic effect between the three bases in the clusters. Hence, for sulfuric acid-base clusters, it is very likely that mixed base clusters with three, or potentially more, bases are involved in the cluster formation pathways. Therefore, quantum chemical studies of sulfuric acid-base clusters involving more than two bases warrant further attention and should be extended to larger systems to allow detailed cluster kinetics modelling.

Author Contributions: Conceptualization, J.E. and H.-B.X.; methodology, J.E. and H.-B.X.; software, J.E.; validation, J.E. and H.-B.X.; formal analysis, J.E.; investigation, J.E. and H.-B.X.; resources, J.E.; data curation, J.E.; writing—original draft preparation, J.E.; writing—review and editing, J.E. and H.-B.X.; visualization, J.E.; supervision, J.E.; project administration, J.E. and H.-B.X.; funding acquisition, J.E. and H.-B.X. All authors have read and agreed to the published version of the manuscript.

Funding: This research was funded by the Independent Research Fund Denmark grant number 9064-00001B. Hong-Bin thanks the National Natural Science Foundation of China (21876024).

Institutional Review Board Statement: Not applicable.

Informed Consent Statement: Not applicable.

Data Availability Statement: Not applicable.

Acknowledgments: The numerical results presented in this work were obtained at the Centre for Scientific Computing, Aarhus http://phys.au.dk/forskning/cscaa/ (accessed on 27 September 2021).

Conflicts of Interest: The authors declare no conflict of interest.

References

1. Haywood, J.; Boucher, O. Estimates of the Direct and Indirect Radiative Forcing due to Tropospheric Aerosols: A Review. *Rev. Geophys.* **2000**, *38*, 513–543. [CrossRef]
2. Lohmann, U.; Feichter, J. Global indirect aerosol effects: A review. *Atmos. Phys. Chem.* **2005**, *5*, 715–737. [CrossRef]
3. Merikanto, J.; Spracklen, D.V.; Mann, G.W.; Pickering, S.J.; Carslaw, K.S. Impact of nucleation on global CCN. *Atmos. Chem. Phys.* **2009**, *9*, 8601–8616. [CrossRef]
4. Kulmala, M.; Kontkanen, J.; Junninen, H.; Lehtipalo, K.; Manninen, H.E.; Nieminen, T.; Petäjä, T.; Sipilä, M.; Schobesberger, S.; Rantala, P.; et al. Direct Observations of Atmospheric Aerosol Nucleation. *Science* **2013**, *339*, 943–946. [CrossRef]
5. Sipilää, M.; Berndt, T.; Petäjä, T.; Brus, D.; Vanhanen, J.; Stratmann, F.; Patokoski, J.; Mauldin, R.L.; Hyvärinen, A.P.; Lihavainen, H.; Kulmala, M. The Role of Sulfuric Acid in Atmospheric Nucleation. *Science* **2010**, *327*, 1243–1246. [CrossRef] [PubMed]
6. Kurtén, T.; Sundberg, M.R.; Vehkamäki, H.; Noppel, M.; Blomqvist, J.; Kulmala, M. Ab Initio and Density Functional Theory Reinvestigation of Gas-Phase Sulfuric Acid Monohydrate and Ammonium Hydrogen Sulfate. *J. Phys. Chem. A* **2006**, *110*, 7178–7188. [CrossRef] [PubMed]
7. Kurtén, T.; Torpo, L.; Sundberg, M.R.; Kerminen, V.; Vehkamäki, H.; Kulmala, M. Estimating the NH_3:H_2SO_4 Ratio of Nucleating Clusters in Atmospheric Conditions using Quantum Chemical Methods. *Atmos. Chem. Phys.* **2007**, *7*, 2765–2773. [CrossRef]
8. Torpo, L.; Kurtén, T.; Vehkamäki, H.; Laasonen, K.; Sundberg, M.R.; Kulmala, M. Significance of Ammonia in Growth of Atmospheric Nanoclusters. *J. Phys. Chem. A* **2007**, *111*, 10671–10674. [CrossRef]

9. Herb, J.; Nadykto, A.B.; Yu, F. Large Ternary Hydrogen-bonded Pre-nucleation Clusters in the Earth's Atmosphere. *Chem. Phys. Lett.* **2011**, *518*, 7–14. [CrossRef]
10. Kirkby, J.; Curtius, J.; Almeida, J.; Dunne, E.; Duplissy, J.; Ehrhart, S.; Franchin, A.; Gagne, S.; Ickes, L.; Kürten, A.; et al. Role of Sulphuric Acid, Ammonia and Galactic Cosmic Rays in Atmospheric Aerosol Nucleation. *Nature* **2011**, *476*, 429–433. [CrossRef]
11. Almeida, J.; Schobesberger, S.; Kürten, A.; Ortega, I.K.; Kupiainen-Määttä, O.; Praplan, A.P.; Adamov, A.; Amorim, A.; Bianchi, F.; Breitenlechner, M.; et al. Molecular Understanding of Sulphuric Acid-Amine Particle Nucleation in the Atmosphere. *Nature* **2013**, *502*, 359–363. [CrossRef] [PubMed]
12. Ge, X.; Wexler, A.S.; Clegg, S.L. Atmospheric Amines-Part I. A Review. *Atmos. Environ.* **2011**, *45*, 524–546. [CrossRef]
13. Jen, C.N.; McMurry, P.H.; Hanson, D.R. Stabilization of Sulfuric acid Dimers by Ammonia, Methylamine, Dimethylamine, and Trimethylamine. *J. Geophys. Res. Atmos.* **2014**, *119*, 7502–7514. [CrossRef]
14. Kurtén, T.; Loukonen, V.; Vehkamäki, H.; Kulmala, M. Amines are Likely to Enhance Neutral and Ion-induced Sulfuric Acid-water Nucleation in the Atmosphere More Effectively than Ammonia. *Atmos. Chem. Phys.* **2008**, *8*, 4095–4103. [CrossRef]
15. Loukonen, V.; Kurtén, T.; Ortega, I.K.; Vehkamäki, H.; Pádua, A.A.H.; Sellegri, K.; Kulmala, M. Enhancing Effect of Dimethylamine in Sulfuric Acid Nucleation in the Presence of Water-A Computational Study. *Atmos. Chem. Phys.* **2010**, *10*, 4961–4974. [CrossRef]
16. Nadykto, A.B.; Yu, F.; Jakovleva, M.V.; Herb, J.; Xu, Y. Amines in the Earth's Atmosphere: A Density Functional Theory Study of the Thermochemistry of Pre-Nucleation Clusters. *Entropy* **2011**, *13*, 554–569. [CrossRef]
17. Nadykto, A.B.; Herb, J.; Yu, F.; Xu, Y. Enhancement in the Production of Nucleating Clusters due to Dimethylamine and Large Uncertainties in the Thermochemistry of Amine-Enhanced Nucleation. *Chem. Phys. Lett.* **2014**, *609*, 42–49. [CrossRef]
18. Nadykto, A.B.; Herb, J.; Yu, F.; Xu, Y.; Nazarenko, E.S. Estimating the Lower Limit of the Impact of Amines on Nucleation in the Earth's Atmosphere. *Entropy* **2015**, *17*, 2764–2780. [CrossRef]
19. Glasoe, W.A.; Volz, K.; Panta, B.; Freshour, N.; Bachman, R.; Hanson, D.R.; McMurry, P.H.; Jen, C. Sulfuric Acid Nucleation: An Experimental Study of the Effect of Seven Bases. *J. Geophys. Res. Atmos.* **2015**, *120*, 1933–1950. [CrossRef]
20. Jen, C.N.; Bachman, R.; Zhao, J.; McMurry, P.H.; Hanson, D.R. Diamine-Sulfuric Acid Reactions are a Potent Source of New Particle Formation. *Geophys. Res. Lett.* **2016**, *43*, 867–873. [CrossRef]
21. Elm, J.; Jen, C.N.; Kurtén, T.; Vehkamäki, H. Strong Hydrogen Bonded Molecular Interactions between Atmospheric Diamines and Sulfuric Acid. *J. Phys. Chem. A* **2016**, *120*, 3693–3700. [CrossRef] [PubMed]
22. Elm, J.; Passananti, M.; Kurtén, T.; Vehkamäki, H. Diamines Can Initiate New Particle Formation in the Atmosphere. *J. Phys. Chem. A* **2017**, *121*, 6155–6164. [CrossRef] [PubMed]
23. Ma, F.; Xie, H.; Elm, J.; Shen, J.; Chen, J.; Vehkamäki, H. Piperazine Enhancing Sulfuric Acid-Based New Particle Formation: Implications for the Atmospheric Fate of Piperazine. *Environ. Sci. Technol.* **2019**, *53*, 8785–8795. [CrossRef] [PubMed]
24. Olenius, T.; Kupiainen-Määttä, O.; Ortega, I.K.; Kurtén, T.; Vehkamäki, H. Free Energy Barrier in the Growth of Sulfuric Acid-Ammonia and Sulfuric Acid-Dimethylamine Clusters. *J. Chem. Phys.* **2013**, *139*. [CrossRef]
25. Elm, J. Elucidating the Limiting Steps in Sulfuric Acid-Base New Particle Formation. *J. Phys. Chem. A* **2017**, *121*, 8288–8295. [CrossRef]
26. Myllys, N.; Kubečka, J.; Besel, V.; Alfaouri, D.; Olenius, T.; Smith, J.N.; Passananti, M. Role of Base Strength, Cluster Structure and Charge in SulfuricAcid-Driven Particle Formation. *Atmos. Chem. Phys.* **2019**, *19*, 9753–9768. [CrossRef]
27. Temelso, B.; Morrison, E.F.; Speer, D.L.; Cao, B.C.; Appiah-Padi, N.; Kim, G.; Shields, G.C. Effect of Mixing Ammonia and Alkylamines on Sulfate Aerosol Formation. *J. Phys. Chem. A* **2018**, *122*, 1612–1622. [CrossRef]
28. Myllys, N.; Chee, S.; Olenius, T.; Lawler, M.; Smith, J. Molecular-Level Understanding of Synergistic Effects in Sulfuric Acid–Amine–Ammonia Mixed Clusters. *J. Phys. Chem. A* **2019**, *123*, 2420–2425. [CrossRef]
29. Li, H.; Ning, A.; Zhong, J.; Zhang, H.; Liu, L.; Zhang, Y.; Zhang, X.; Zeng, X.C.; He, H. Influence of Atmospheric Conditions on Sulfuric Acid-dimethylamine-ammonia-based New Particle Formation. *Chemosphere* **2020**, *245*, 125554. [CrossRef]
30. Frisch, M.J.; Trucks, G.W.; Schlegel, H.B.; Scuseria, G.E.; Robb, M.A.; Cheeseman, J.R.; Scalmani, G.; Barone, V.; Petersson, G.A.; Nakatsuji, H.; et al. *Gaussian 16 Rev. A.03 Release Notes*; Gaussian, Inc.: Wallingford, CT, USA, 2016. Available online: https://gaussian.com/relnotes_a03/ (accessed on 27 September 2021).
31. Elm, J. An Atmospheric Cluster Database Consisting of Sulfuric Acid, Bases, Organics, and Water. *ACS Omega* **2019**, *4*, 10965–10974. [CrossRef]
32. Riplinger, C.; Neese, F. An Efficient and Near Linear Scaling Pair Natural Orbital Based Local Coupled Cluster Method. *J. Chem. Phys.* **2013**, *138*, 034106. [CrossRef] [PubMed]
33. Riplinger, C.; Sandhoefer, B.; Hansen, A.; Neese, F. Natural Triple Excitations in Local Coupled Cluster Calculations with Pair Natural Orbitals. *J. Chem. Phys.* **2013**, *139*, 134101. [CrossRef] [PubMed]
34. Neese F. The ORCA program system. *WIREs Comput. Mol. Sci.* **2012**, *2*, 73–78. [CrossRef]
35. Neese, F. Software update: the ORCA program system, version 4.0. *Wiley Interdiscip. Rev. Comput. Mol. Sci.* **2017**, *8*, e1327. [CrossRef]
36. Funes-Ardois, I.; Paton, R. GoodVibes: GoodVibes v1.0.1; 2016. Available online: https://github.com/patonlab/GoodVibes (accessed on 27 September 2021).
37. Grimme, S. Supramolecular Binding Thermodynamics by Dispersion-corrected Density Functional Theory. *Chem. Eur. J.* **2012**, *18*, 9955–9964. [CrossRef] [PubMed]

38. Elm, J.; Kubečka, J.; Besel, V.; abd R. Halonen, M.J.J.; Kurtén, T.; Vehkamäki, H. Modeling the Formation and Growth of Atmospheric Molecular Clusters: A Review. *J. Aerosol. Sci.* **2020**, *149*, 105621. [CrossRef]
39. Smith, J.N.; Draper, D.C.; Chee, S.; Dam, M.; Glicker, H.; Myers, D.; Thomas, A.E.; Lawler, M.J.; Myllys, N. Atmospheric Clusters to Nanoparticles: Recent Progress and Challenges in Closing the Gap in Chemical Composition. *J. Aerosol. Sci.* **2021**, *153*, 105733. [CrossRef]
40. Elm, J.; Bilde, M.; Mikkelsen, K.V. Assessment of Binding Energies of Atmopsheric Clusters. *Phys. Chem. Chem. Phys.* **2013**, *15*, 16442–16445. [CrossRef]
41. Elm, J.; Kristensen, K. Basis Set Convergence of the Binding Energies of Strongly Hydrogen-Bonded Atmospheric Clusters. *Phys. Chem. Chem. Phys.* **2017**, *19*, 1122–1133. [CrossRef]
42. Schmitz, G.; Elm, J. Assessment of the DLPNO binding energies of strongly non-covalent bonded atmospheric molecular clusters. *ACS Omega* **2020**, *5*, 7601–7612. [CrossRef]
43. Kubečka, J.; Besel, V.; Kurtén, T.; Myllys, N.; Vehkamäki, H. Configurational sampling of noncovalent (atmospheric) molecular clusters: Sulfuric acid and guanidine. *J. Phys. Chem. A* **2019**, *123*, 6022–6033. [CrossRef]
44. Odbadrakh, T.T.; Gale, A.G.; Ball, B.T.; Temelso, B.; Shields, G.C. Computation of Atmospheric Concentrations of Molecular Clusters from ab initio Thermochemistry. *J. Vis. Exp.* **2020**, *158*, e60964. [CrossRef] [PubMed]
45. Elm, J. Clusteromics I: Principles, Protocols and Applications to Sulfuric Acid-Base Cluster Formation. *ACS Omega* **2021**, *6*, 7804–7814. [CrossRef]
46. Elm, J. Clusteromics II: Methanesulfonic Acid-Base Cluster Formation. *ACS Omega* **2021**, *6*, 17035–17044. [CrossRef]
47. Temelso, B.; Mabey, J.M.; Kubota, T.; Appiah-Padi, N.; Shields, G.C. ArbAlign: A Tool for Optimal Alignment of Arbitrarily Ordered Isomers Using the Kuhn–Munkres Algorithm. *J. Chem. Inf. Model* **2017**, *57*, 1045–1054. [CrossRef] [PubMed]
48. Kildgaard, J.V.; Mikkelsen, K.V.; Bilde, M.; Elm, J. Hydration of Atmospheric Molecular Clusters: A New Method for Systematic Configurational Sampling. *J. Phys. Chem. A* **2018**, *122*, 5026–5036. [CrossRef] [PubMed]
49. Hunter, E.P.L.; Lias, S.G. Evaluated Gas Phase Basicities and Proton Affinities of Molecules: An Update. *J. Phys. Chem. Ref. Data* **1998**, *27*, 413. [CrossRef]
50. Chen, H.H.; Varner, M.E.; Gerber, R.B.; Finlayson-Pitts, B.J. Reactions of methanesulfonic acid with amines and ammonia as a source of new particles in air. *J. Phys. Chem. B* **2016**, *120*, 1526–1536. [CrossRef] [PubMed]
51. Shen, J.; Elm, J.; Xie, H.; Chen, J.; Niu, J.; Vehkamäki, H. Structural Effects of Amines in Enhancing Methanesulfonic Acid-Driven New Particle Formation. *Environ. Sci. Technol.* **2020**, *54*, 13498–13508. [CrossRef]
52. Kürten, A.; Jokinen, T.; Simon, M.; Sipilä, M.; Sarnela, N.; Junninen, H.; Adamov, A.; Almeida, J.; Amorim, A.; Bianchi, F.; et al. Neutral Molecular Cluster Formation of Sulfuric Acid-Dimethylamine Observed in Real Time under Atmospheric Conditions. *Proc. Natl. Acad. Sci. USA* **2014**, *111*, 15019–15024. [CrossRef]